



The Manufacturing Engineering Society International Conference, MESIC 2015

## Geometrical verification based on a laser triangulation system in industrial environment. Effect of the image noise in the measurement results

F.J. Brosed<sup>a,\*</sup>, J.J. Aguilar<sup>a</sup>, J. Santolaria<sup>a</sup>, R. Lázaro<sup>a</sup>

<sup>a</sup>*Dpto. Ing. de Diseño y Fabricación, E.I.N.A. Universidad de Zaragoza, C/María de Luna nº 3, 50018, Zaragoza, Spain*

---

### Abstract

The use of laser triangulation systems is widely spread in industrial applications, especially in industrial metrology. These applications are usually affected by external perturbations, in particular, image noise and reflections can be an important error source for these kinds of sensors when high precision is required or when the scanning task is developed in an industrial environment. This research is focused in the improvement of the behavior of a laser triangulation sensor working with high noise images. The aim of the image analysis technique is to avoid or reduce the effect of the background noise on the measurement results (flatness). The analysis technique is tested with images captured in the industrial environment of the measurement system. The results show a proper behavior of the algorithm with high noise component images and the feasibility of the technique for use in the inspection of 100% of the production.

© 2015 Published by Elsevier Ltd. This is an open access article under the CC BY-NC-ND license (<http://creativecommons.org/licenses/by-nc-nd/4.0/>).

Peer-review under responsibility of the Scientific Committee of MESIC 2015

*Keywords:* Precision industrial measurement; Image analysis; Laser line detection; Weighted average method;

---

### 1. Introduction

The use of laser triangulation systems is widely spread in industrial applications, especially in industrial metrology [1]. These applications are usually affected by external perturbations, in particular, image noise and reflections can be an important error source for these kinds of sensors when high precision is required or when the

---

\* Corresponding author. Tel.: +3 487 676 5456; fax: +3 497 676 2235.  
E-mail address: [fjbrosed@unizar.es](mailto:fjbrosed@unizar.es)

scanning task is developed in an industrial environment. Several techniques are used to extract 3D geometry data from a laser sensor [2, 3], but most of them, especially those used with laser triangulation sensors, need to run an algorithm for laser detection in images [4-6]. Laser line detection has been a basic problem of computer vision and has become a significant source of error when a laser triangulation system is applied to high precision measurement tasks [7]. The centre of mass method has been found to provide the best results when the laser stripe detection is carried out in an industrial environment, as in the case presented in this work [8, 9]. In this paper an algorithm for laser detection is presented and tested with high noise component images. The proposed method is performed in three steps: detection of the laser stripe using a centre of gravity technique; dynamic adjustment of the mask size to improve the accuracy [10] using the grey level of the pixels in the mask; and finally, detection of peaks due to reflections or noise in the image by using a first order polynomial, because the laser stripe projected over the inspected object is supposed to be very close to a straight line (high precision flatness measurement).

The aim of the presented work is to improve the functionality of a measurement system applied to the geometrical inspection of 100% of production. The measurement system is a laser triangulation sensor mounted in a motion linear stage (MLS) to scan surfaces. A robotic arm is used to locate the surface to be verified in the field of view of the laser sensor. The verification process is carried out in an industrial environment where the captured images show a high noise component.

### Nomenclature

d	Maximum admissible distance between a detected point and the laser line
den	Mean value of the grey level in the mask
it	Maximum value of iterations
L	Lower Limit of illumination
m	Full size of the mask [pixels]
$m_{\min}$	Minimum size for the mask [pixels]
s	Half the size of the mask [pixels]
t	Threshold for the detection of laser in image
U	Upper Limit of illumination
(u,v)	Image coordinates [pixels]
$v_0$	Central pixel of the mask
$v_{WA}$	Subpixel coordinate in v direction resulting from the basic weighted average method
$v_{sp\_1}$	Subpixel coordinate in v direction after apply the threshold
$v_{sp\_2}$	Subpixel coordinate in v direction after apply the noise detection algorithm
$w_{v0+i}$	Grey level of the pixel with v coordinate $v=v_{0+i}$

## 2. Measurement system and application

The measurement system is composed of a laser triangulation sensor (LTS) mounted in a motorized linear system (MLS) to scan surfaces. Fig. 1a shows the components and a scheme of the measurement process of the system. The LTS is made up of a camera and a laser diode with an optic pattern that generates a plane that illuminates the scene. The intersection between the laser plane and the surface to be measured generates a laser line. The laser line is captured by the camera and the images are analysed in order to extract the laser line image coordinates (2D coordinates:  $u, v$ ). The LTS calibration makes it possible to transform the image coordinates of the laser line points into coordinates of the global 3D frame of the system ( $x, y, z$ ). The cloud of points obtained from the surface scan is treated mathematically to extract the geometrical characteristics of the surface. Finally a robotic arm is used to handle the measured parts. The resolution of the system is 0.1mm/pixel in X (approx.  $u$  direction), 0.18mm/pixel in Y (MLS direction) and 0.8mm/pixel in Z coordinate (approx.  $v$  direction). A more detailed description of the components, the design of the measurement system, the measurement procedure, and the measurement results can be found in [7].

The study has been carried out using a reference part of a model that is habitually verified with the system. The reference part is a heat exchanger with a single surface to be verified. The surface of the heat exchanger is a sheet-metal flat surface of  $100 \times 180\text{mm}$  with eight holes manufactured by punching. Five of them (7.50mm in diameter) are clamping holes. The last three holes (18mm in diameter) are holes for the circulation of the refrigeration fluids. The bottom of these three holes presents a flat annular surface (4mm in width) located at a depth of 4mm (Fig. 1b). The flat annular region and the wall of the hole will generate undesired illumination of the scene due to reflection of the laser.

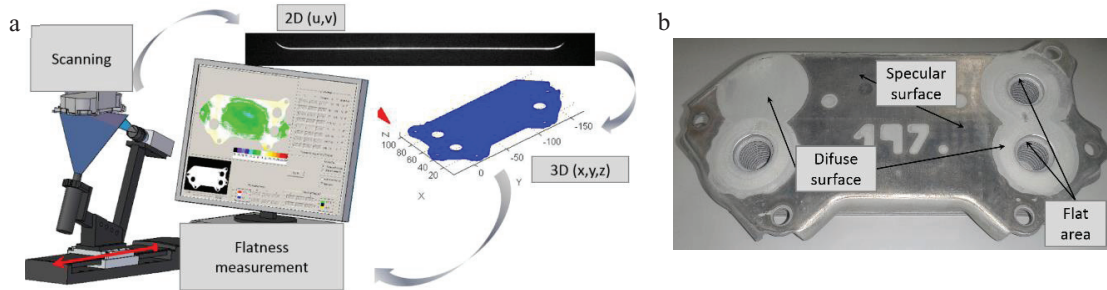


Fig. 1. (a) The LTS scans the surface under inspection (lower surface of the part in the gripper). Two-dimensional coordinates of the laser line in the captured images are extracted and a cloud of points (3D) is obtained after applying the calibration data. The cloud of points is treated mathematically to obtain a measurement result for the flatness. (b) Surface areas and details of the part under inspection

The flat surface of the heat exchanger presents regions where the laser reflection on the surface is almost specular and other adjacent areas where the reflection is almost diffuse.

When the reflection of the laser on the surface is almost specular, the contrast of the laser line with the background decreases and the pixels of the laser line present a grey level under 255 (grey level scale from 0 to 255). On the other hand, when the reflection of the laser is almost diffuse, the pixels of the laser line in the image present a grey level of 255; often more than one pixel per column appears with a grey level of 255.

In the first case (specular reflection), point loss could occur, and in the second one (diffuse reflection), the accuracy of detection of the laser line could be affected and undesired illumination of the surface could occur when the laser illuminates elements such as hole walls or threads, Fig. 2.

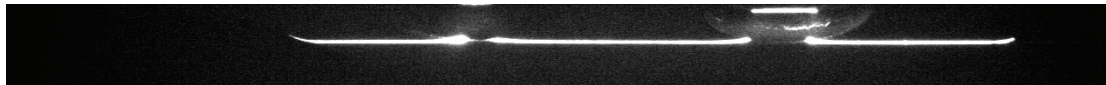


Fig. 2. Captured image of the heat exchanger. Flat surface near the refrigeration fluid holes where the noise level is higher due to the illumination of the bottom and the wall of the hole

### 3. Laser line detection and subpixel estimation

The aim of the proposed algorithm is to extract the subpixel coordinate of the centre of the laser stripe avoiding the effect of the noise in image. Three steps are used to extract the subpixel coordinates of the laser: first step is to detect the laser stripe. The second is to adjust the mask size to improve the accuracy. And the third step is to detect peaks due to noise and undesired illumination. The methods and different variations for each step are described in the next subsections.

#### 3.1. Detection algorithm

The detection of the laser stripe is carried out using a centre of gravity technique. The laser line is close to horizontal in the image (u coordinate constant in the image), so the laser detection algorithm is applied for each

column individually. The method used to estimate the line centre is the weighted average (WA) of the data (1), which is widely used in subpixel location estimation [11].

$$v_{WA} = \frac{\sum_{i=-s}^s w_{v_0+i} \cdot (v_0 + i)}{\sum_{i=-s}^s w_{v_0+i}} \tag{1}$$

Where, for each column of pixels in an image:  $v_{WA}$  is the WA (centre of mass) of the data, subpixel  $v$  coordinate of the centre of the estimated laser line;  $v_0$  is the  $v$  coordinate of the centre of the considered mask;  $m=2 \cdot s$  is the size of the mask and  $w_{v_0+i}$  is the grey level of the pixel with  $v$  coordinate  $v=v_0+i$ . This method, following several iterations, works properly to estimate the subpixel coordinate of the laser line in the column ( $v$  coordinate) when the noise component of the image is acceptable: the grey level of the background noise is clearly differentiated from the grey level of the laser pixels. But when the level of noise in the image increases, the results show a deviation from the laser line (Fig. 3)

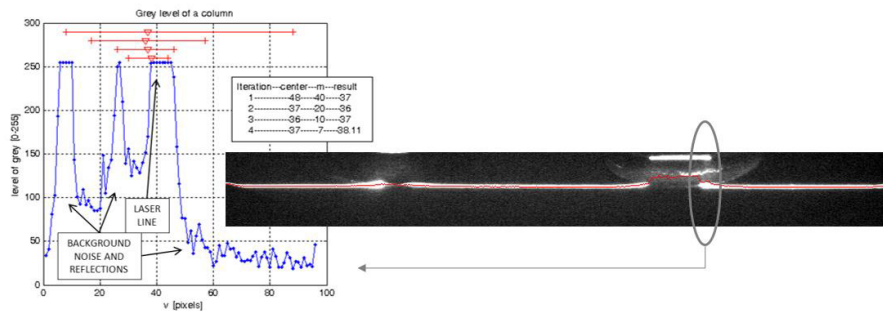


Fig. 3. Effect of the noise on the subpixel estimation. The reflections on the edges of the surface generate a non-uniform background noise. Reflections can be observed too. The result of the subpixel estimation is displaced from the centre of the laser line due to the noise. The red line in the image captured shows the results of the subpixel estimation for the whole image.

WA is usually applied with the assumption that the laser line will always be found, but in industrial environments it is necessary to check the presence of the laser in the column [8]. In this case, a threshold for the mean value of the grey level in the mask is settled. An initial estimation of the subpixel coordinate of the laser line in a column of the image ( $v_{sp\_1}$ ) can be obtained using (1) and (2), where  $t$  is the threshold and  $den$  is the mean value of the grey level in the mask.

$$v_{sp\_1} = \begin{cases} v_{WA} & \text{if } den > t \\ 0 & \text{if } den \leq t \end{cases}; \quad den = \frac{\sum_{i=-s}^s w_{v+t}}{2s + 1} \tag{2}$$

Obtaining the subpixel estimation of the laser stripe with this method may be inaccurate, depending on the noise characteristics of the image. Because the centre of mass of the column can be displaced by non-uniform distributed noise (Fig. 3). This effect can be decreased by selecting an adequate mask size, as is explained in the next subsection.

### 3.2. Mask size selection

An iterative method that changes the mask size depending on the intensity has been used to avoid the effect of non-uniform distributed noise. This method consists in evaluating the illumination of the mask ( $den$ ) and changing the mask size of the next iteration. An initial value of the mask,  $m$ , is defined and the subpixel value is calculated by applying (1) centred in  $v_{sp\_1}$ . The size of the mask is changed following the flow chart shown in Fig. 4. Two values

of illumination, Upper Limit ( $U$ ) and Lower Limit ( $L$ ), are defined; if the value of den is between them, the iterative process stops, if den is higher than  $U$ , the size of the mask increases, and if den is lower than  $L$ , the size of the mask decreases. A maximum value of iterations ( $it$ ) is defined to avoid an infinite loop and a minimum size of the mask,  $m_{min}$ , is defined too. The lower the number of pixels of background noise included in the mask, the more accurate the subpixel estimation will be (Fig. 4).  $U$ ,  $L$ , and its values can be adjusted to decrease the influence of non-uniform distributed noise in the image. Subpixel estimation ( $v_{sp\_2}$ ) for each value of  $v_{sp\_1}$  is obtained for the same image as that used in Fig. 4. The results of applying the proposed method to a column of an image are depicted and the result of the subpixel estimation for the whole image is presented (Fig. 4).

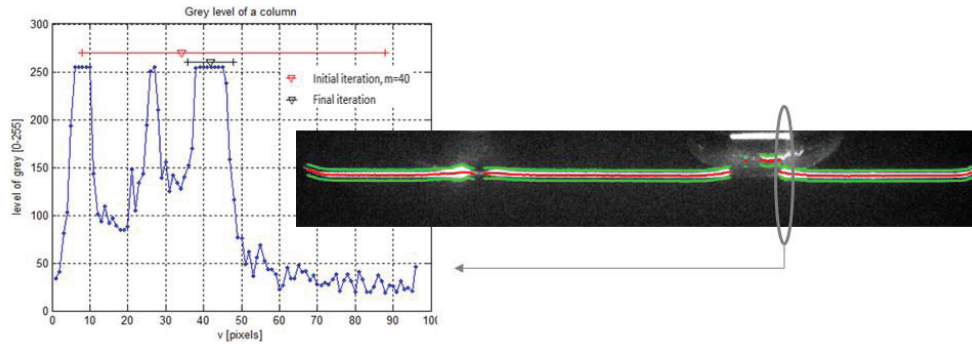


Fig. 4. Dynamic selection of the size of the mask. The graph shows the grey level of a column of an image from the surface scan. The laser line appears between  $v = 35$  pixels and  $v = 45$  pixels. The background noise shows a non-uniform distribution. Reflections can be observed too. The red line in the image captured shows the results of the subpixel estimation and the size of the last mask for the laser line.

### 3.3. Noise peaks detection

The laser detection and the method of mask size selection, which are applied consecutively, can result in failure when there is undesired illumination in the image. Overall, if the undesired illumination has high levels of intensity (Fig. 5). This method is presented to detect peaks due to undesired illumination that have passed through the previous steps (Subsections 3.1 and 3.2). The laser stripe can be described by a straight line, almost in the region of interest, that is, on the flat surface of the heat exchanger. So, a straight line is fitted (Least Squares method) with the points ( $v_{sp\_2}$ : 2D coordinates) extracted from the previous two steps. If the distance of a point ( $u$ ,  $v_{sp\_2}$ ) from the straight line is higher than a threshold value,  $d$ , then that point is eliminated from the data. This method avoids the incorporation of spurious points in the flatness measurement.

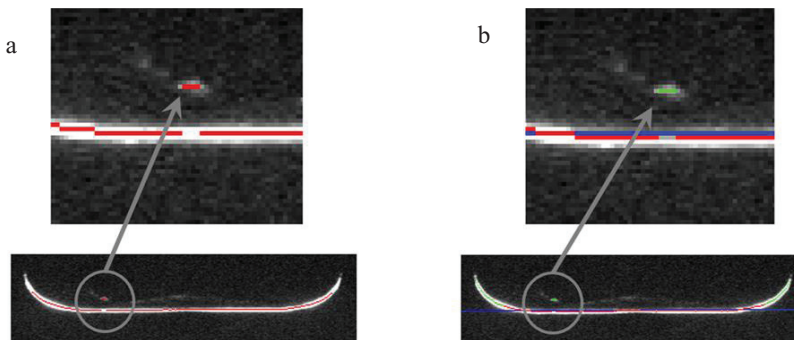


Fig. 5. (a) Input data for the noise peak detection method; undesired illumination peaks are detected. (b) Output data, the detected noise peaks are filtered. The red dots are the subpixel estimation results and the blue dots represent the line fitted with the input data.

Most of the images taken work correctly without this third step, but correct detection of the peaks outside the laser line helps to avoid inaccuracies in the measurement results when a high noise component appears.

Fig. 6 shows a case of undesired illumination. The light point outside the laser line appears on the boundary surface of the region to be measured (Fig. 5). If the light point is not detected and segmented, the flatness error can increase (0.08mm/px) but, after applying the detection of the peaks due to noise in the image, the points outside the laser line are filtered (Fig. 5).

This noise peak detection method works properly when analysing images from a flat surface, which is the case of the application. This can be observed on the left and right edges of the laser line (Fig. 5b). These edges show curves and the points that are outside the flat area under inspection are rejected (green points) for the flatness verification. A more general application can be obtained using collinear union segments or using a higher degree polynomial fitting procedure. Anyway, the shape of the laser in the image should always be known in order to apply this third step of the proposed method.

#### 4. Results and discussion

The results shown in this section are focused on the way in which the noise in the image affects the laser detection and the subpixel estimation of the laser line centre. However, the influence on the measurement results is described in the last subsection in order to illustrate the importance of correct laser detection and subpixel estimation.

##### 4.1. Image analysis

Several flat surfaces have been scanned and the images from the scan have been analysed using the method explained in Section 3. The performance of the proposed algorithm is shown in Fig. 6 (red line), where an image is exposed and the subpixel estimation of the laser line is depicted. These results are compared with those obtained by applying the WA method iteratively (green line), decreasing the mask size in fixed steps (as it is shown in Fig. 3). Finally the results are compared with those obtained by applying the basic WA algorithm (1) once to each column of the image (blue line).

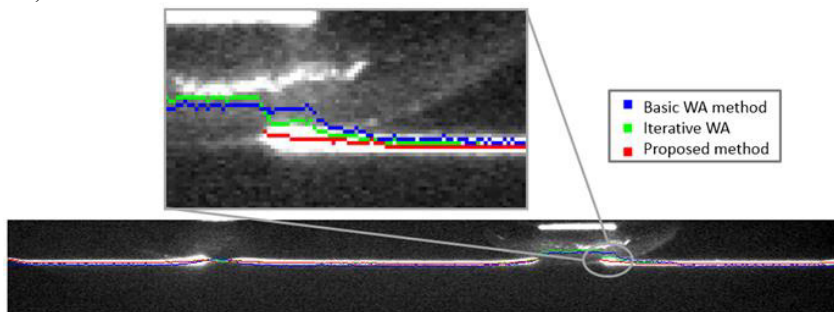


Fig. 6. Subpixel estimation results. Results of the method proposed in this work (red line) compared with the results obtained with the initial method used by the measurement system (green line) and also compared with the results obtained after applying the basic WA method (applying WA once in each column, blue line).

The mask size has been chosen so that the pixels inside it are only those of the laser line and those in the boundary between the laser and the background so that the effect of noise in the image is avoided. The results of the basic WA method appear to be biased toward the lower saturation boundary of the laser. This happens because there are more pixels below the laser line than above it (49 VS 35 pixels) and, although the background noise is similar, as the mask size includes almost the whole column, the noise below the laser line contains the results of the basic WA method close to the saturation boundary of the laser line. This situation is only avoided when the background noise of the upper area increases (near the holes).

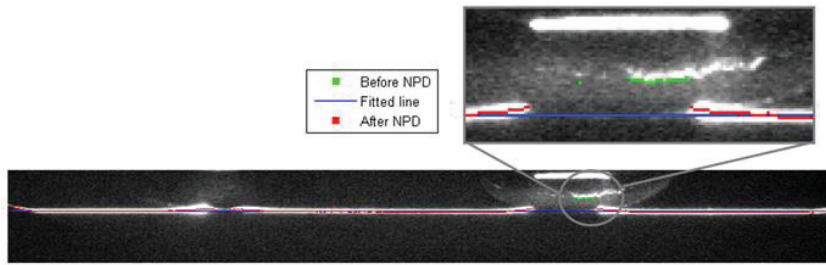


Fig. 7. The subpixel estimation results of the method proposed in this work: After applying the noise peak detection method (after NPD, red line) and before applying the NPD. The line fitted to detect the noise peaks is shown too

The first two steps of the proposed method (Subsections 3.1 and 3.2) can result in failure to detect peaks that do not correspond to the laser line. These points, corresponding to undesired illumination, should be detected and eliminated although they will only appear in some cases in which reflections generate high intensity peaks (Fig. 7). The procedure described in Subsection 3.3 is applied to detect the points away from the fitted line and to avoid the effect of the peaks of noise on the measurement results

#### 4.2. Measurement results

The present work is focused on the effect of noise in the image on the subpixel estimation of the laser line. However, the transmission of the errors in laser detection and subpixel estimation affects the measurement results of the system. The measurement result obtained after applying the initial method is shown in Fig. 8. Some peaks due to reflections and undesired illumination can be observed in the centre of the surface and near the fluid circulation holes. These irregularities are smoothed and the peaks due to reflections are detected and eliminated after applying the proposed method (Fig. 8).

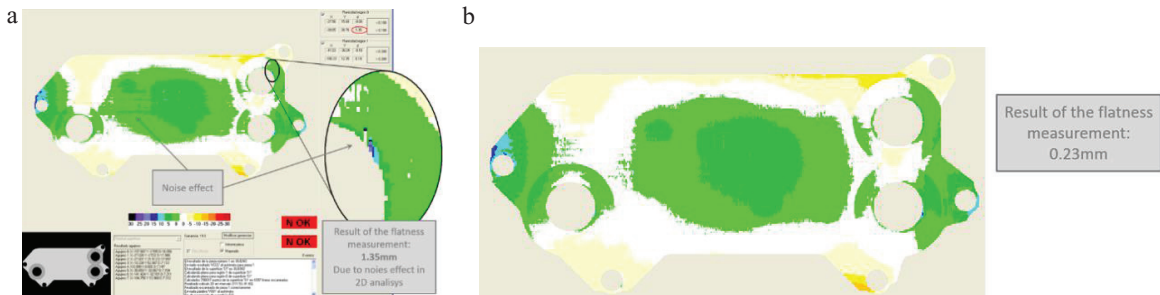


Fig. 8. (a) Measurement results with the iterative WA. (b) Measurement results with the proposed method

The proposed algorithm allows flatness verification of the part with a cycle time similar to that used with the initial algorithm. The image analysis begins once an image has been captured without waiting for the scan to be completed, and therefore the time limit for completion of the image analysis is 20s (scan time). The calculation time for the image analysis of all the captured images (1300) is under that limit. So, the proposed method is suitable for verification of 100% of the production and can therefore be used by the laser sensor.

## 5. Conclusions

Two major effects have been found after the analysis of the effect of the background noise on the image analysis results: displacement of the subpixel estimation and detection of spurious points. An algorithm has been proposed from the study of the effect of the noise. An iterative process based on the WA method has been developed to avoid the displacement of the subpixel estimation. In each iteration, the size of the mask changes depending on the laser characteristics in the image. The last step of the method is the fitting of a line with all the laser points that have been detected in order to eliminate spurious points.

The proposed algorithm sets out the steps taken to avoid the consideration of reflections or undesired illumination as part of the scanned surface, which would generate incorrect measurement results. The proposed method has been tested with actual images and measurement results have been obtained, proving that the method is suitable for a 100% production verification process.

## Acknowledgements

This work has been funded by CICYT (Spanish Governmental Research Agency) under project DPI2007-61513.

## References

- [1] Bi, Z.M.; Wang, L. Advances in 3D Data Acquisition and Processing for Industrial Applications. *Robot. Comput. Integrated Manuf.* 2010, 26, 403-413.
- [2] Savio, E.; De Chiffre, L.; Schmitt, R. "Metrology of freeform shaped parts". *Annals of the CIRP* 2007, 56(2), 810-835.
- [3] Kumar, S. M.; Smith, M. L.; Smith, L. N.; Midha, S. "An Overview of Passive and Active Vision Techniques for and-Held 3D Data Acquisition". *Proc. of SPIE* 2003, 4877.
- [4] Brink, W.; Robinson, A.; Rodrigues, M. "Indexing Uncoded Stripe Patterns in Structured Light Systems by Maximum Spanning Trees". *Proceedings of the British Machine Conference* 2008, 57, 1-10.
- [5] Robinson, A.; Alboul, L.; Rodrigues, M. "Methods for Indexing Stripes in Uncoded Structured Light Scanning Systems". *Journal of WSCG* 2004, 12(1-3).
- [6] Deng, F.; Fung, K. S. M.; Deng, J.; Lam, E. Y. "An edge detection algorithm based on rectangular Gaussian kernels for machine vision applications" *Proc. SPIE* 7251, *Image Processing: Machine Vision Applications II*, 72510N (3 February 2009); doi: 10.1117/12.805241.
- [7] Brosed, F. J.; Aguilar, J. J.; Guillomía, D.; Santolaria, J. "3D Geometrical Inspection of Complex Geometry Parts Using a Novel Laser Triangulation Sensor and a Robot". *Sensors* 2011, 11, 90-110.
- [8] Haug, K.; Pritschow, G. "Robust laser-stripe sensor for automated weld-seam-tracking in the shipbuilding industry". *Industrial Electronics Society*, 1998. *IECON '98. Proceedings of the 24th Annual Conference of the IEEE* 1998, 2, 1236-1241 vol.2.
- [9] Fisher, R. B.; Naidu, D. K. "A Comparison of Algorithms for Subpixel Peak Detection" *Image Technology, Advances in Image Processing, Multimedia and Machine Vision*, 1996, pp. 385, 404, Springer-Verlag.
- [10] Ta, H.; Kim, D.; Lee, S. "A novel laser line detection algorithm for robot application", *Control, Automation and Systems (ICCAS)*, 2011 11th International Conference on; vol., no., pp.361, 365, 26-29 Oct. 2011.
- [11] Kim, D.; Lee, S.; Kim, H.; Lee, S. "Wide-angle laser structured light system calibration with a planar object". *Control Automation and Systems (ICCAS)*, 2010 International Conference on 2010, 1879-1882